INSTITUTE OF PHYSICS PUBLISHING JOURNAL OF PHYSICS: CONDENSED MATTER

J. Phys.: Condens. Matter **16** (2004) 5453–5459 PII: S0953-8984(04)78669-5

Optimized basis sets for the collinear and non-collinear phases of iron

V M García-Suárez[1], C M Newman[2], C J Lambert[2], J M Pruneda[3] and J Ferrer[1]

[1] Departamento de Física, Universidad de Oviedo, 33007, Oviedo, Spain
[2] Department of Physics, Lancaster University, Lancaster, LA1 4YB, UK
[3] Department of Earth Sciences, University of Cambridge, Cambridge CB2 3EQ, UK

E-mail: victor@condmat.uniovi.es

Received 30 March 2004
Published 16 July 2004
Online at stacks.iop.org/JPhysCM/16/5453
doi:10.1088/0953-8984/16/30/008

Abstract

Systematic implementations of density functional calculations of magnetic materials, based on atomic orbitals basis sets, are scarce. We have implemented in one such code the ability to compute non-collinear arrangements of the spin moments in the GGA approximation, including spiral structures. We have also made a thorough study of the degree of accuracy of the energy with the size of the basis and the extent of the orbitals. We have tested our results for the different phases of bulk iron as well as for small clusters of this element. We specifically show how the relative stability of the different competing states changes with the degree of completeness of the basis, and present the minimal set which provides reliable results.

(Some figures in this article are in colour only in the electronic version)

Molecular dynamics packages based on density functional theory (DFT) [1] represent a specially useful set of tools in the theoretical analysis of materials. Most approaches use plane waves as a basis set, which allows a great degree of accuracy provided the number of plane waves is large enough, and use all the electrons in the atom to describe core and valence states. However, these approximations are numerically very expensive and do not scale linearly with the number of atoms. Other approaches, such as SIESTA, implement the tight-binding philosophy [2], using norm-conserving pseudopotentials [3], to integrate away core energy levels, and very flexible basis sets (BS) made up of numerical atomic-like wavefunctions to handle valence electrons. Assessment of the degree of reliability of those BS might be essential, since competing would-be ground states may in some instances have small energy differences. Such analyses have already been performed for selected molecules and solids [4, 5]. Those studies show how both the number of wavefunctions (WF) used as well as their extent are variational parameters, providing therefore a path for systematic improvements

of the accuracy of a simulation [4]. A similar study for magnetic elements or materials seems to be highly desirable, since they have their own peculiarities and, in particular, are usually tougher to simulate. We have performed an exhaustive study of the degree of accuracy of the basis for iron in most of its bulk phases as well as for small clusters. We find that SIESTA provides a highly accurate description of the systems we have scrutinized, provided that a sizeable number of extended orbitals is used.

In order to simulate all the magnetic phases of iron we have implemented in SIESTA the possibility to cope with non-collinear commensurate spin structures in the GGA approximation, since non-collinear LDA, already included in this package, fails to provide adequate ground states and lattice constants of a number of magnetic transition metals. Due to the fact that the energy functional $f(\hat{n}, \vec{\nabla}\hat{n})$ is only known for collinear magnets, it is necessary to rotate the density matrix $\hat{n}$ at every point $\vec{r}$ to the collinear reference frame, where it is diagonal. In this case we have also to deal with the gradient, so that there are two possibilities previous to the calculation of the XC energy and potential: (1) we can diagonalize the density matrix, $\hat{n} \rightarrow \hat{n}_{\mathrm{d}} = \hat{U}^{\dagger}\hat{n}\hat{U}$, and then calculate the gradient of it, $\vec{\nabla}\hat{n}_{\mathrm{d}}$, or (2) we can rotate both the density matrix and its gradient:

$$\hat{n}, \vec{\nabla}\hat{n} \rightarrow \hat{n}_{\mathrm{d}}, \hat{U}^{\dagger}(\vec{\nabla}\hat{n})\hat{U} \tag{1}$$

and then select only the diagonal matrix elements of the gradient-density matrix. The second approach was previously used by Sandratskii and co-workers [6]. We have verified analytically that these two approaches are identical to linear order in gradients. We have also implemented them in the code and obtained the same results in both cases.

We have included the possibility to simulate non-commensurate spiral structures of pitch vector $\vec{q}$ [7, 8]. To do so we have used the generalized Bloch theorem [7], so that our wavefunction has the following form:

$$\hat{\psi}_{\vec{k},\vec{q}} = \sum_{\vec{R},\mu} \mathrm{e}^{-\mathrm{i}\vec{k}\cdot\vec{R}_{\mu}} \phi_{\mu}(\vec{r} - \vec{R}_{\mu}) \hat{U}_{z}^{\dagger}(\vec{q}\cdot\vec{r}) \hat{U}_{y}^{\dagger}(\theta) \begin{pmatrix} c_{\vec{k},\mu,\uparrow} \\ c_{\vec{k},\mu,\downarrow} \end{pmatrix} \tag{2}$$

where $\vec{R}_{\mu} = \vec{R} - \vec{d}_{\mu}$ ($\vec{d}_{\mu}$ goes to atoms in the same unit cell) and $\hat{U}$ are rotation matrices, with $\vec{q}\cdot\vec{r}$ and θ the azimuthal and polar angles, respectively.

Choice of pseudopotentials and integration grids. SIESTA includes norm-conserving pseudopotentials [3] optimized so that their local part is smooth [2]. We have used for iron the pseudopotential proposed by Izquierdo and co-workers [9], generated from the atomic configuration $[\mathrm{Ar}]3\mathrm{d}^{7}4\mathrm{s}^{1}$, with core radii for 4s, 4p, 3d and 4f orbitals set equal to 2.00 au and the radius for the partial-core to 0.7 au.

Since the energy of the different states need not shift rigidly when increasing accuracy and, moreover, competing ground states for (fcc) iron have energy differences as tiny as 2–3 meV, we decided to set the number of k points, the grid cutoff (maximum kinetic energy of the plane waves that can be represented in the real-space integration grid without aliasing) and the electronic temperature to match an accuracy of about 1 meV. Figure 1 shows typical results for the convergence of the free energy of bcc ferromagnetic iron as a function of those parameters. We find then that we need up to 4000 k points, 700 Ryd (which corresponds to about 50.000 points in the real space integration grid) and a temperature smaller than 300 K to meet the desired accuracy.

Choice of basis set. SIESTA allows for a large flexibility in the use of BS of WF which describe valence electrons. For each species of atom, one may specify one shell of s, p, d and f orbitals (or not). Within each shell, one may choose how many WF having the required angular symmetry are needed. A single-zeta basis (SZ) is equivalent to choosing just one WF. Completion of the basis leads to double-zeta and triple-zeta bases (DZ, TZ). In addition, one

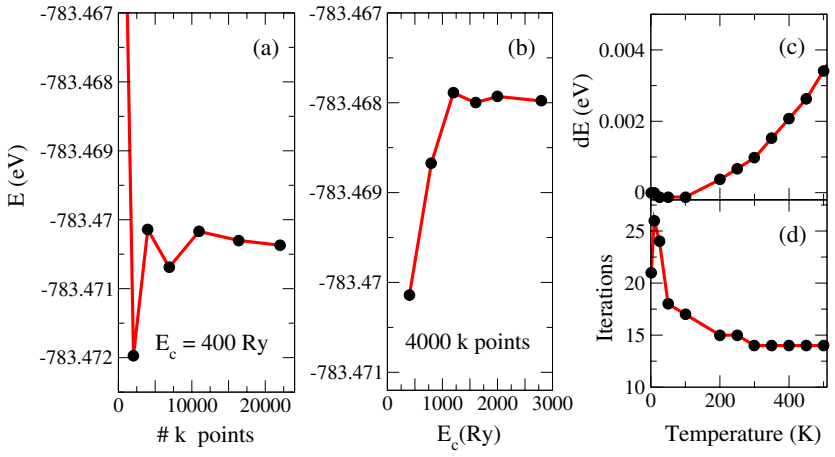

Figure 1. Total free energy of bcc ferromagnetic iron as a function of (a) number of k points in half the Brillouin zone (with a grid cutoff of 400 Ryd (27.000 points)) and (b) grid cutoff (with 4000 k points in half the Brillouin zone). (c) Energy relative to the case $T \approx 0$ and (d) number of iterations needed to achieve convergence as a function of the electronic temperature, calculated with 4000 k points and a grid cutoff of 400 Ryd. An optimized DZ basis was used.

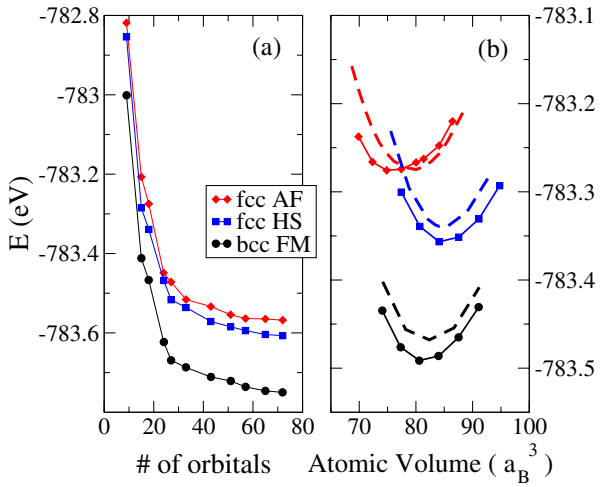

Figure 2. (a) Evolution of the free energy of the three most stable states of iron as a function of the size of the BS. AF = antiferromagnetic, HS = ferromagnetic high spin and FM = ferromagnetic. (b) Cohesive energy curves of those same three states for the two minima found using the BSD. The discontinuous curves correspond to radii of 6 au and the continuous to 10 au. The calculations have been performed using the GGA approximation.

may polarize an orbital (P), which means adding WF which correspond to one higher angular momentum unit [2]. Using more WF is equivalent to filling up the Hilbert space and provides a better variational estimate of the ground state. The minimum basis required to accommodate the eight valence electrons of iron would be SZ for both s and d orbitals, which provide a total of 6 WF per spin.

We have minimized a few BS ranging from SZ–SZ–SZ (9 WF) to TZTP–TZTP–TZTP (72 WF). Figure 2(a) shows the convergence of the energy, calculated using GGA, for the three

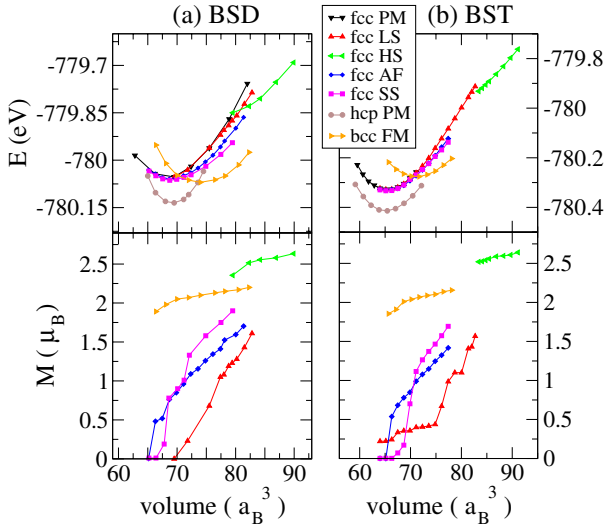

Figure 3. Free energy and magnetic moment of the ground and lowest excited states of bulk iron as predicted by LDA approximation, using (a) BSD and (b) BST, as a function of the atomic volume. PM = paramagnetic, AF = antiferromagnetic, LS = ferromagnetic low-spin, HS = ferromagnetic high-spin, SS = spin spiral and FM = ferromagnetic.

most stable states of bulk iron, e.g. bcc ferromagnetic, fcc ferromagnetic high-spin and fcc antiferromagnetic as a function of the number of orbitals used in the BS. Notice that at least 30 WF are needed to achieve converged energy differences among the three states.

Radii of basis orbitals. We have paid special attention to the minimization of two bases: BS DZP–SZ–DZ (BSD, 18 WF) and TZ–TZ–TZ (BST, 27 WF), where we have used a grid software program to look for local minima of the energy as a function of the radii of the first zeta of s, p and d orbitals. For the BSD basis we obtain a first local minimum for somewhat confined radii of about 6 au and a deeper one for radii of about 10 au. Figure 2(b) shows that extended radii improve both the energy and the lattice constant substantially. For instance, the lattice constant a_0 of the bcc ferromagnetic state obtained using BSD in the GGA approximation, as predicted by the first minimum, is 2.90 Å, while the second one provides a better estimate, $a_0 = 2.88$ Å. In contrast, the energy landscape for the BST basis is very flat for radii s, p and d from 6 to 10 au. Such a result was expected, since completion of the basis should lead to weaker dependences on cutoff radii.

Results for iron in the LDA. We find that a DZP BS predicts erroneous orderings of the ground and first excited states. Figure 3(a) shows that the ferromagnetic bcc state is more stable that the paramagnetic fcc one. Figure 3(b) shows that usage of a more complete BS corrects such a double error. We find then that it is necessary to use at least a BST in order to obtain good predictions of the different physical magnitudes. The lattice constant, magnetic moment and bulk modulus of ferromagnetic bcc iron are found to be 2.76 Å, 2.08 μ_B and 2.68 Mbar with such a BST, which compare extremely well with the best all-electron plane-wave calculations [10]. Moreover, the lattice constant for paramagnetic fcc, 3.38 Å, is also very similar to the all-electron estimate of 3.375 Å, while the energy difference between both states is somewhat underestimated (55 versus about 70–80 meV) [10].

We turn now to the predictions for the spiral state. Tsunoda found that fcc iron stabilized in the form of nanometre-sized pellets inside a Cu matrix, with a lattice constant of 3.577 Å and

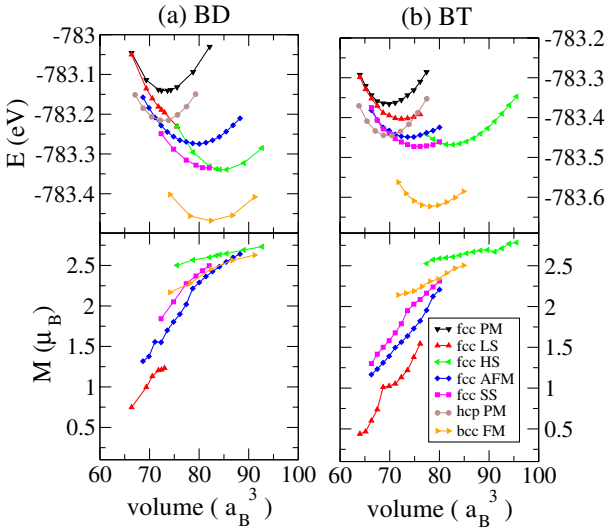

Figure 4. Free energy and magnetic moment of the ground and lowest excited states of bulk iron as predicted by the GGA approximation, using (a) BSD and (b) BST as a function of the atomic volume.

a spiral spin ordering of pitch $\vec{q}_0 = 2\pi/a \times (0.12, 0, 1)$ [11]. We scan the energy as function of pitch vector along the ΓX and XW directions, where we find two minima $\vec{q}_1 = 2\pi/a \times (0, 0, 0.6)$ (S1) and $\vec{q}_2 = 2\pi/a \times (0.2, 0, 1)$ (S2); this last one being very close to $\vec{q}_0$. The energy curves for lattice constants equal or larger than 3.58 Å only have the $\vec{q}_1$ minimum. The second minimum appears when we decrease a at or below 3.54 Å, becoming lowest in energy at $a \approx 3.50$ Å.

Results for iron in GGA. DZP basis sets also provide poor results in the GGA approximation, even though the relative stability of the lowest energy states is correct now, see figure 4. We find that the relative position of the energy curves of the fcc states change significantly when we increase the size of the basis from BSD to BST. We have therefore further increased the size of the BS to obtain more accurate results: we have included more polarization orbitals of p, d and f symmetry up to 72 WF, and have found that the energy of the three curves is essentially converged (see figure 2) for the BST basis. We obtain an equilibrium lattice constant, magnetic moment and bulk modulus of 2.85 Å, 2.31 μ_B and 1.83 Mbar, respectively, for the ground state, which compare reasonably well with former all-electron or ultrasoft-pseudopotentials-based plane wave calculations [12, 6, 13].

The results for spiral structures in the GGA approximation for lattice constants ranging from 3.47 to 3.56 Å are summarized in figure 5. It can be seen that the free energy curves change rather more again when we increase the size of the basis, since the shape of the energy parabolae as a function of atomic volume also change significantly (see figure 4). For the BST, the ferromagnetic high-spin state has a considerably high energy and there is a clear asymmetric double-well structure with activation barriers of at least 7 meV. We find that the S2 state has already clearly developed when $a = 3.52$ Å, but the ground state is S1 down to lattice constants of 3.47 Å. We predict that the most stable fcc state has a spiral spin arrangement and a lattice constant of 3.56 Å, very close to the experimental value 3.577 Å [11] (see figure 4).

Marsman and Hafner [13] have also performed a thorough study of the spiral structures of fcc lattices with tetrahedric, orthorhombic and monoclinic distortions using the non-collinear

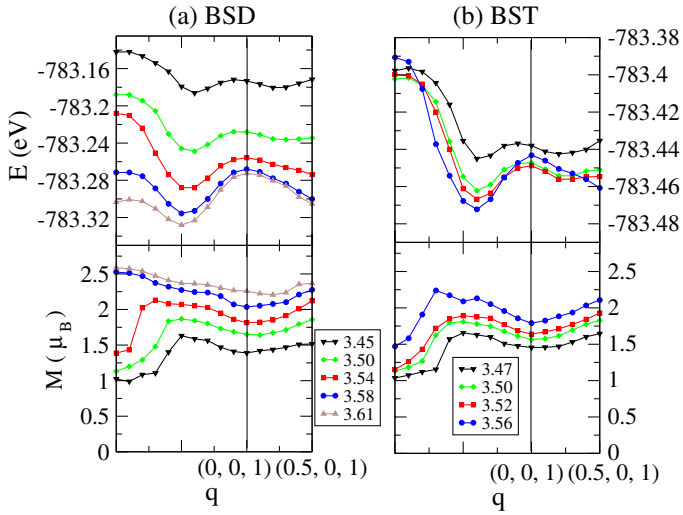

Figure 5. Free energy and magnetic moment as a function of pitch vector $\vec{q}$ of the spiral state for different lattice constants ranging from 3.48 to 3.61 Å for (a) BSD and (b) BST.

Table 1. Bond lengths a (Å), binding energy per atom E_b (eV/atom) and total magnetic moment M (μ_B) for iron clusters of up to five atoms calculated with a BST and the GGA.

	a (Å)	B (eV Å^{-1})	M (μ_B)
Fe_2	2.02	1.51	6.00
Fe_3 $D_{\infty h}$	2.28	1.72	5.62
Fe_3 C_{3v}	2.27	1.88	10.00
Fe_4 C_{4v}	2.30	2.21	14.00
Fe_4 T_d	1, 2 ↔ 3, 4 2.27	2.31	14.00
	1 ↔ 2, 3 ↔ 4 2.65		
Fe_5 D_{3h}	1 ↔ 2, 3 2 ↔ 3 2.43	2.58	17.07
	1, 2, 3 ↔ 4, 5 2.37		

GGA. In the undistorted case they found the same results we have obtained using the non-collinear LDA: their absolute minimum corresponds to a spiral state S2, but its equilibrium lattice constant, $a = 3.49$ Å, is much smaller than the experimental one. On the contrary, we find that the most stable fcc state is a S1 spiral with equilibrium lattice constant $a = 3.56$ Å, much closer to experiments. They also found that the equilibrium constant of their (metastable) S1 state was 3.51 Å.

Finally, in order to test the transferability of our parameters, we have also simulated clusters with a number of atoms of iron ranging from 2 to 5, using the non-collinear GGA and a BST. Our results compare very well with previous theoretical calculations [16, 15, 9, 17, 14], and even improve upon them when comparisons are made with the experimental values found for the Fe_2 cluster [18]. Our calculations are shown in table 1.

To summarize, we have performed a thorough study of the diverse phases of iron using a DFT code based on localized wavefunctions. We have therefore:

(1) determined the minimal basis set of optimized wave functions required to obtain reliable results,
(2) implemented in the code the non-collinear GGA and the ability to compute uncommensurate spin spiral arrangements and

(3) found that the most stable fcc state has a lattice constant of 3.56 Å and a spiral arrangement of spins of pitch vector $\vec{q}_1 = 2\pi/a \times (0, 0, 0.6)$.

Acknowledgments

JF wishes to thank to the authors and developers of the SIESTA code for a number of helpful discussions and e-mail exchanges: P Ordejón, J Soler, E Artacho, A García-Arribas and J Junquera. He also wishes to acknowledge discussions with A Vega and S Bouarab. Optimization of the BS was carried out with the use of the package INNERGRID which was generously supplied by GRID SYSTEMS. The work presented here has been funded by the Spanish MCyT and the European Union under project no. BFM2000-0526 and contract no. HPRN-CT-2000-00144, respectively. VMGS thanks the Spanish Ministerio Español de Educación, Cultura y Deporte for a fellowship.

References

[1] Kohn W and Sham L J 1965 *Phys. Rev.* **140** A1133
[2] Soler J M *et al* 2002 *J. Phys.: Condens. Matter* **14** 2745
[3] Troullier N and Martins J L 1991 *Phys. Rev.* B **43** 1993
[4] Junquera J, Paz O, Sánchez-Portal D and Artacho E 2001 *Phys. Rev.* B **64** 235111
[5] Anglada E, Soler J M, Junquera J and Artacho E 2002 *Phys. Rev.* B **66** 205101
[6] Knopfle K, Sandratskii L M and Kubler J 2000 *Phys. Rev.* B **62** 5564
[7] Sandratskii L M 1988 *Adv. Phys.* **47** 91
[8] Sticht J, Hock K H and Kubler J 1989 *J. Phys.: Condens. Matter* **1** 8155
[9] Izquierdo J *et al* 2000 *Phys. Rev.* B **61** 13639
[10] Wang C S, Klein B F and Krakauer H 1985 *Phys. Rev. Lett.* **54** 1852
[11] Tsunoda Y 1989 *J. Phys.: Condens. Matter* **1** 10427
[12] Moroni E G, Kresse G, Hafner J and Furtmuller J 1997 *Phys. Rev.* B **56** 15629
[13] Marsman M and Hafner J 2002 *Phys. Rev.* B **66** 224409
[14] Postnikov A V, Entel P and Soler J M 2003 *Eur. Phys. J.* D **25** 261
[15] Hobbs D, Kresse G and Hafner J 2000 *Phys. Rev.* B **62** 11556
[16] Oda T, Pasquarello A and Carr R 1998 *Phys. Rev. Lett.* **80** 3622
[17] Diéguez O *et al* 2001 *Phys. Rev.* B **63** 205407
[18] Purdum H, Montano P A, Shenoy G K and Morrison T 1982 *Phys. Rev.* B **25** 4412